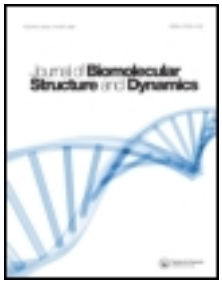

Journal of Biomolecular Structure and Dynamics
Publication details, including instructions for authors and subscription information:
http://www.tandfonline.com/loi/tbsd20

Role of N-terminal residues on folding and stability of C-phycoerythrin: simulation and urea-induced denaturation studies

Khalid Anwer[a], Ravi Sonani[b], Datta Madamwar[b], Parvesh Singh[c], Faez Khan[c], Krishna Bisetty[c], Faizan Ahmad[a] & Md. Imtaiyaz Hassan[a]

[a] Centre for Interdisciplinary Research in Basic Sciences, Jamia Millia Islamia (A Central University), Jamia Nagar, New Delhi 110 025, India

[b] BRD School of Biosciences, Sardar Patel University, Vallabh Vidyanagar, Gujarat 388 120, India

[c] Department of Chemistry, Durban University of Technology, Durban 4000, South Africa

Published online: 27 Nov 2013.

To cite this article: Khalid Anwer, Ravi Sonani, Datta Madamwar, Parvesh Singh, Faez Khan, Krishna Bisetty, Faizan Ahmad & Md. Imtaiyaz Hassan , Journal of Biomolecular Structure and Dynamics (2013): Role of N-terminal residues on folding and stability of C-phycoerythrin: simulation and urea-induced denaturation studies, Journal of Biomolecular Structure and Dynamics, DOI: 10.1080/07391102.2013.855144

To link to this article: http://dx.doi.org/10.1080/07391102.2013.855144

Journal of Biomolecular Structure and Dynamics, 2013
http://dx.doi.org/10.1080/07391102.2013.855144

Role of N-terminal residues on folding and stability of C-phycoerythrin: simulation and urea-induced denaturation studies

Khalid Anwer[a], Ravi Sonani[b], Datta Madamwar[b], Parvesh Singh[c], Faez Khan[c], Krishna Bisetty[c], Faizan Ahmad[a] and Md. Imtaiyaz Hassan[a]*

[a]*Centre for Interdisciplinary Research in Basic Sciences, Jamia Millia Islamia (A Central University), Jamia Nagar, New Delhi 110 025, India;* [b]*BRD School of Biosciences, Sardar Patel University, Vallabh Vidyanagar, Gujarat 388 120, India;* [c]*Department of Chemistry, Durban University of Technology, Durban 4000, South Africa*

Communicated by Ramaswamy H. Sarma

(*Received 14 August 2013; accepted 9 October 2013*)

The conformational state of biliproteins can be determined by optical properties of the covalently linked chromophores. Recently determined crystal structure of truncated form of α-subunit of cyanobacterial phycoerythrin (αC-PE) from *Phormidium tenue* provides a new insight into the structure–function relationship of αC-PE. To compare their stabilities, we have measured urea-induced denaturation transitions of the full length αC-PE (FL-αC-PE) and truncated αC-PE (Tr-αC-PE) followed by observing changes in absorbance at 565 nm, fluorescence at 350 and 573 nm, and circular dichroism at 222 nm as a function of [urea], the molar concentration of urea. The transition curve of each protein was analyzed for ΔG_D^0, the value of Gibbs free energy change on denaturation (ΔG_D) in the absence of urea; *m*, the slope ($=\partial\Delta G_D/\partial[\text{urea}]$), and C_m, the midpoint of the denaturation curve, i.e. [urea] at which $\Delta G_D = 0$. A difference of about 10% in ΔG_D^0 observed between FL-αC-PE and Tr-αC-PE, suggests that the two proteins are almost equally stable, and the natural deletion of 31 residues from the N-terminal side of the full length protein does not alter its stability. Furthermore, normalization of probes shows that the urea-induced denaturation of both the proteins is a two-state process. Folding of both structural variants (Tr-αC-PE and FL-αC-PE) of *P. tenue* were also studied using molecular dynamics simulations at 300 K. The results show clearly that the stability of the proteins is evenly distributed over the whole structure indicating no significant role of N-terminal residues in the stability of both proteins.

Keywords: biliproteins; C-phycoerythrin; chromophore; protein denaturation; folding and stability; molecular dynamics; AMBER

Introduction

Studies based upon unfolding and refolding of the native and unfolded proteins using various theoretical and experimental approaches provided different insights into how proteins fold (Ma, Xie, Zhang, & Zhao, 2007). Despite a huge amount of effort since the last 4–5 decades, prediction of protein structures still remains an unsolved problem (Griogoriev, 1998). Practical use of modeling and simulation of known sequences and structures of proteins have been enhancing our understanding of the protein folding problem (Griogoriev, 1998). Different models of molecular dynamics (MD) and simulation can be applied to all α-helical proteins of known 3-D structures like cyanobacterial phycoerythrin (C-PE) to demonstrate high prediction accuracy in comparison with other known models (Griogoriev, 1998).

Cyanobacteria are the most primordial among oxygenic photosynthetic organisms, and their antenna system consists of characteristic phycobiliproteins (PBPs), categorized as phycoerythrin (PE), phycocyanin (PC), and allophycocyanin (APC) forming a supramolecular assembly called phycobilisomes (PBS) (Gray, Lipschultz, & Gantt, 1973; MacColl, 1998, 2004). PB is a light harvesting pigment of antennae of photosystem II in cyanobacteria, red algae, and cryptophytes. These protein complexes are anchored to thylakoid membranes, which are made of stacks of PBPs and their associated linker polypeptides (Cornejo, Beale, Terry, & Lagarias, 1992). Each PB consists of a core made of APC to which several outwardly oriented rods made of stacked disks of PC, and PE or phycoerythrocyanin are attached (Glazer, 1982; Gray et al., 1973). The energy transfer in the organism proceeds successively in the direction from PE → PC → APC → chlorophyll *a*, with an overall efficiency of almost 100% (MacColl, 1998, 2004; Yokono, Akimoto, Koyama, Tsuchiya, & Mimuro, 2008). The lights absorbed by PBPs are in the regions of visible

*Corresponding author. Email: mihassan@jmi.ac.in

spectrum where chlorophyll *a* has lower efficiency. The spectral properties of PBPs are mainly governed by their prosthetic groups, which are linear tetrapyrolles known as phycobilin including phycocyanobilin, phycoerythrobilin, phycourobilin, and phycobiliviolin. Interestingly, spectral properties of phycobilins are highly influenced by the protein environment (MacColl, 1998, 1999, 2004).

PE is one of the unique and special accessory light harvesting pigments which exists in the form of hexamer ($\alpha_6\beta_6$) or dimers of trimers $(\alpha_3\beta_3)_2$ in PBS of different blue-green algae, cryptomonads, glaucomonads and red algae (MacColl, 1998). C-PE contains 6α and 6β subunits arranged in ring-like assemblies where the three monomers are present in the three-fold symmetry (Chang et al., 1996; Soni et al., 2010). Each α-subunit of PE consists of 164 residues, while each β-subunit contains 171 residues (MacColl, 1998; Soni et al., 2010). The structure of C-PE resembles with globin proteins which contain two open-chain linear tetrapyrolle chromophores called phycoerythrobilins (PEBs), which are covalently attached with each α-subunit at Cys82 and Cys139. While β-subunit of C-PE contains three PEBs of which two are covalently attached with Cys84 and Cys155, the third chromophore is doubly linked to Cys50 and Cys6 (Chang et al., 1996; MacColl, 1998; Soni et al., 2010). The interactions between PEB with protein atoms as well as protein-chromophore environments are critically responsible for the photon absorption properties of C-PE.

Recently, we have identified and determined the crystal structure of α-subunit of C-PE (αC-PE) from *Phormidium tenue*, which is devoid of 31 residues from its amino terminal side (Soni et al., 2010), as compared to all other α-PEs including that of red algae (α-RPE) *Polysiphonia urceolata* containing complete 164 residues (Chang et al., 1996). It is interesting to note that truncation of 31 residues occur naturally when the organism is grown or kept in prolonged starved condition. However, the truncated αC-PE maintains its light absorbing and photo sensitivity capabilities significantly (Chang et al., 1996; Soni et al., 2010). The full length αC-PE (FL-αC-PE) and truncated αC-PE (Tr-αC-PE) can be used as a model system to understand the role of N-terminal residues in protein folding. Here, we studied the equilibrium, folded state ↔ unfolded state of the full length and truncated αC-PEs induced by urea using absorption, fluorescence, and circular dichroism (CD) measurements. Since the structure of the intact αC-PE is not known, we have used structural information of αR-PE, for the full length α-CPE, Tr-αC-PE and αR-PE have almost identical sequence (94% homology), structure, and function (Chang et al., 1996; Soni et al., 2010).

Two MD simulation methods were performed on αR-PE and Tr-αC-PE to investigate urea-induced folding/unfolding and stability profiles in the presence and absence of N-terminal residues of FL-αC-PE. Due to the challenges involved in identifying the location of 'specific binding sites' of urea on proteins (Modig, Kurian, Prendergast, & Halle, 2003), the presence of urea was omitted during MD simulations of the urea-induced denaturation. Apart from determination of role of 31 N-terminal residues in protein folding and stability, our findings may be helpful to understand the mechanism of survival of this cyanobacterium and other marine algae under stress conditions including starvation, as under these conditions the organism is maintaining its pigment proteins and absorption properties for food preparation and survival. This may again help to grow higher photosynthetic plants under this and similar types of stress environmental conditions.

Experimental Setup

Materials and methods

Urea of ultra pure grade was purchased from MP Biomedicals, LLC (Illkirch, France). Sodium cacodylate trihydrate and Sephadex G-150 matrix were obtained from Sigma-Aldrich (St Louis, USA) and GE Healthcare UK Limited, respectively. Other chemicals were purchased from local suppliers. All chemicals used were of molecular biology research grade.

Isolation and purification

Proteins were isolated and purified from *P. tenue* sp. A27DM collected from rocky shores of Bet Dwarka, Okha, and estuarine mouth of river Daman Ganga (India). The enrichment, provision of growth conditions, extraction, and purification of C-PE were carried out using our well optimized protocol described elsewhere (Parmar, 2011; Parmar, Singh, Kaushal, Sonawala, & Madamwar, 2011; Shah, Garg, & Madamwar, 2001). Briefly, the cyanobacterium was harvested in artificial sea water nutrients, and the cell mass was washed with 1.0 M Tris-HCl buffer (pH 8.1) containing 3.0 mM sodium azide. For the purification of FL-αC-PE and Tr-αC-PE, cultures were harvested when they were young (20 days) as well as when old (90–200 days), respectively. The procedures for getting both types of proteins have already been published (Parmar, 2011; Parmar et al., 2011; Soni et al., 2010). Washed cell mass was resuspended in the same buffer, and repeated freeze–thaw cycles (−30 and 4 °C) were applied for C-PE release. This was followed by two-step (20 and 70%) ammonium sulfate precipitation. The precipitate was dissolved in 10 mM Tris buffer and subjected to the gel (G-150) permeation chromatography column pre-equilibrated with 10 mM Tris buffer. The purity of the purified protein was checked by the native and SDS-PAGE using

silver staining (Parmar, 2010; Parmar et al., 2011; Singh, Parmar, & Madamwar, 2009). The entire purification procedure was carried out in dark at 4 °C. All buffer solutions required above during isolation and purification were prepared in mili-Q water supplemented with .01% sodium azide. Stock solutions of both proteins were stored in the Tris-HCl buffer (pH 8.1) containing .01% sodium azide at 4 °C.

To remove buffer constituents and sodium azide, stock solutions were dialyzed against several changes with .1 M KCl (pH 7.0). The concentration of the dialyzed and filtered stock solutions of FL-αC-PE and Tr-αC-PE were determined experimentally using a value of 265,000 M^{-1} cm^{-1} for the molar absorption coefficient at 565 nm (Pace, 1995).

Sample preparation for denaturation and renaturation experiments

To study the urea-induced denaturation, stock solution of urea was prepared by weight in 50 mM sodium cacodylate buffer (pH 7.0) containing .1 M KCl. However, its concentration (9.0 M) was determined by refractive index measurements (Pace, 1986). Urea solutions were always freshly prepared and used to avoid development of significant concentration of highly reactive cyanate ions upon standing. For the preparation of protein solutions for denaturation and renaturation experiments, the procedure reported earlier was followed (Ahmad & Bigelow, 1982). In brief, for each denaturation experiment, known amounts of the protein stock solution, buffer, and concentrated urea solutions were mixed and incubated for a time long enough to ensure the complete denaturation process. Urea was added in subsequent samples with gradual increase in concentration from .2 to 8.0 M. A similar procedure was employed in preparing the solution for renaturation experiments with the exception that the protein was first denatured by adding required (4, 5, and 6 M) concentration of urea solution and then diluted with the same buffer. The urea-induced denaturation was studied at pH 7.0 and 25 °C. We have always checked the pH of the protein solutions thus prepared.

Measurement of absorption spectra

Absorption spectra of FL-αC-PE and Tr-αC-PE were measured in Jasco UV/visible spectrophotometer (Jasco V-660, Model B 028661152) equipped with peltier-type temperature controller (ETCS-761). All measurements were carried out in the wavelength range 800–250 nm using 1 cm path length cuvettes. The protein concentration used was in the range of .15–.4 mg ml^{-1}. All spectral measurements were done at least three times at 25 ± .1 °C.

Measurement of fluorescence spectra

Fluorescence measurements were carried out in Jasco spectrofluorimeter (Model FP-6200) using 5 mm quartz cuvette. All experiments were carried out at 25 ± .1 °C which is maintained by an external thermostated water circulator. FL-αC-PE and Tr-αC-PE have intrinsic (Trp77) and extrinsic (PEB) fluorophores. To measure Trp77 fluorescence, the protein variants were excited at 287 nm, and emission spectra were recorded in the range of 300–400 nm. To measure the PEB's fluorescence, protein solutions were excited at 479 nm, and emission spectra were recorded in the range 500–600 nm (Royer, 2006). The protein concentration used was .2–.5 mg ml^{-1}.

CD measurements

The far-UV CD measurements of FL-αC-PE and Tr-αC-PE were carried out in Jasco spectropolarimeter (J-715) equipped with peltier type of temperature controller (PTC-348WI). The CD instrument was routinely calibrated with d-10-camphorsulphonic acid. CD spectra of FL-αC-PE and Tr-αC-PE were collected with a response time of 1 s and a scan speed of 100 nm min^{-1}. Each spectrum was an average of at least five scans. All measurements were carried out at 25 ± .1 °C. The far-UV spectra were collected in the wavelength range of 250–200 nm using .1 cm path length cuvette. The protein concentration used was .25–.5 mg ml^{-1}. The raw data at a given wavelength λ (nm) were converted into concentration-independent parameter $[\theta]_\lambda$ (deg $cm^2 dmol^{-1}$), the mean residue ellipticity at λ using the relation,

$$[\theta]_\lambda = M_0\theta_\lambda / 10lc \quad (1)$$

where θ_λ is the observed ellipticity in milli degrees at λ, M_0 is the mean residue weight of the protein, l is the path length of the cell in centimeters, and c is the protein concentration in mg ml^{-1}. It should be noted that each observed $[\theta]_\lambda$ of the protein was corrected for the contribution of the solvent.

Data analysis

The sigmoidal urea-induced denaturation curves (plot of y, the optical property of the protein vs. [urea], the molar concentration of the denaturant) were analyzed for $\Delta G_D{}^0$ (Gibbs free energy change in the absence of urea), m (slope of the plot of ΔG_D, the Gibbs free energy change vs. [urea], i.e. $\partial\Delta G_D/\partial$[urea]), and C_m (midpoint of denaturation curve, i.e. [urea] at which $\Delta G_D = 0$). This analysis involves a least-squares method to fit the entire data of a denaturation curve, according to the relation,

$$y = y_N + y_D \times \mathrm{Exp}[-(\Delta G_D^0 - m[\mathrm{urea}])/\mathrm{RT}]/ (1 + \mathrm{Exp}[-(\Delta G_D^0 - m[\mathrm{urea}])/\mathrm{RT}]) \quad (2)$$

where y_N and y_D are properties of the native (N) and denatured (D) protein molecules under the same experimental condition in which y has been measured, R is gas constant, and T is the temperature in Kelvin (K). It should be noted that Equation (2) assumes that a plot of ΔG_D vs. [urea] is linear, and the dependencies of y_N and y_D on [urea] are also linear (i.e. $y_N = a_N + b_N$ [urea], $y_D = a_D + b_D$ [urea], where a_N, b_N, a_D and b_D are [urea]-independent parameters, and subscripts N and D signify that parameters are for the native and denatured states, respectively). The denatured fraction of the protein, f_D in a given [urea] was determined using the relation,

$$f_D = (y - y_N)/(y_D - y_N) = y - (a_N + b_N[\mathrm{urea}])/(a_D - a_N + b_D - b_N)[\mathrm{urea}] \quad (3)$$

MD method

The MD simulations for both proteins (Tr-αC-PE and FL-αC-PE) were performed at molecular mechanics level using the AMBER 9.0 program (Case et al., 2005). Both proteins were soaked in the box of water molecules with dimensions 65.419, 82.631, and 61.996 Å (for Tr-αC-PE) and 92.915, 77.969, and 58.302 Å (for FL-αC-PE) using the tleap module of AMBER. The total number of water molecules added in case of Tr-αC-PE and FL-αC-PE were 8,136 and 10,513, respectively. The charges on both proteins were neutralized by the addition of two Na^+ ions to maintain neutrality. The system was then minimized using 1000 steps of steepest descent, followed by a subsequent minimization using the conjugate gradient algorithm until a convergence criteria of .001 kcal mol^{-1} Å was observed. The temperature of both systems was subsequently raised from 0 to 300 K during their equilibration period (200 ps) at a constant volume under periodic boundary conditions. After the first equilibration phase, the particle-mesh Ewald method (Horng et al., 2005) was applied, and the production phase consisting of 5 ns was performed for each system at 300 K under these conditions. Each snapshot of the conformation was stored after 1 ps during the sampling process. The analysis of each MD trajectory was performed using the PTRAJ module in AMBER.

Results and discussion

PE is an essential photosynthetic pigment for cyanobacteria, red algae, and glaucophytes, thriving in high salt concentration of marine environment (Wilbanks et al., 1991). C-PE was found to maintain its 3-D structure and function in harsh conditions and extreme environments. Here, our aim is to understand the role of the N-terminal residues in the folding and stability of FL-αC-PE and Tr-αC-PE. To achieve that, we have carried out *in vitro* and *in silico* studies of the urea-induced denaturation of both proteins using conformational techniques and MD simulations.

Generation of natural variants of αC-PE

Ideally, αC-PE from *P. tenue* is composed of 19 and 20 kDa α- and β-subunits, respectively. We have observed that both α- and β-subunits are synthesized properly but showing different patterns of degradation depending upon the duration of culture (Soni et al., 2010). In the fresh culture conditions, we observed the production of the full length αC-PE and full length βC-PE. On the other hand, under prolonged nutritional starvation condition, a truncation of the first 31 N-terminal residues in αC-PE occurs giving a distinct form, Tr-αC-PE that contains residues from 32–164. While βC-PE is found to be completely degraded under such conditions and such species were not isolated. The reason for the degradation is not known except that such truncation/degradation occurs to fulfill the nitrogen needs of the organism for its survival (Soni et al., 2010).

Long-term storage of purified C-PE which exists as a hexamer ($\alpha_6\beta_6$) causes natural degradation leaving truncated Tr-αC-PE only. It is interesting to see that Tr-αC-PE is found to be highly stable, and no further degradation takes place even after long-term storage. The difference in molecular masses of the full length (19 kDa) and truncated (14 kDa) forms of αC-PE was clearly observed by gel electrophoresis.

Structural and thermodynamic characterizations

Figure 1(a) shows visible absorbance spectra of the native and denatured FL-αC-PE and Tr-αC-PE at pH 7.0 (50 mM sodium cacodylate containing .1 M KCl) and 25 ± .1 °C. It is seen in this figure that FL-αC-PE gives a broad peak in the region 600–450 nm having a maximum at 565 nm, whereas in case of Tr-αC-PE this broad peak splits into two peaks with maxima at 566 and 542 nm with a trough at 550 nm. This difference was used to check whether or not the FL-αC-PE is intact. The λ_{max} of both proteins are very similar, there is only a slightly increased and a minor hypsochromic (red-shift) in Tr-αC-PE. Since chromophores are covalently attached to Cys82 and Cys139, both proteins are showing absorption maxima near 565 nm, suggesting no significant difference in their light absorption activity. It has been argued that this absorption by both proteins is due to the interaction between the folded polypeptide chain and the

two thioether bonded PEBs (Parmar, 2011; Parmar et al., 2011). This argument was based on the fact that the apoprotein does not absorb in the visible region, and PEB has a very low absorbance (MacColl, 1998, 2004). These findings suggest that the folding/unfolding reactions of FL-αC-PE and Tr-αC-PE can be followed by observing changes in the visible absorption at 565 nm.

To see the effect of urea on the structural stability of FL-αC-PE and Tr-αC-PE, we have measured the absorption spectra of both proteins in the range 800–250 nm as

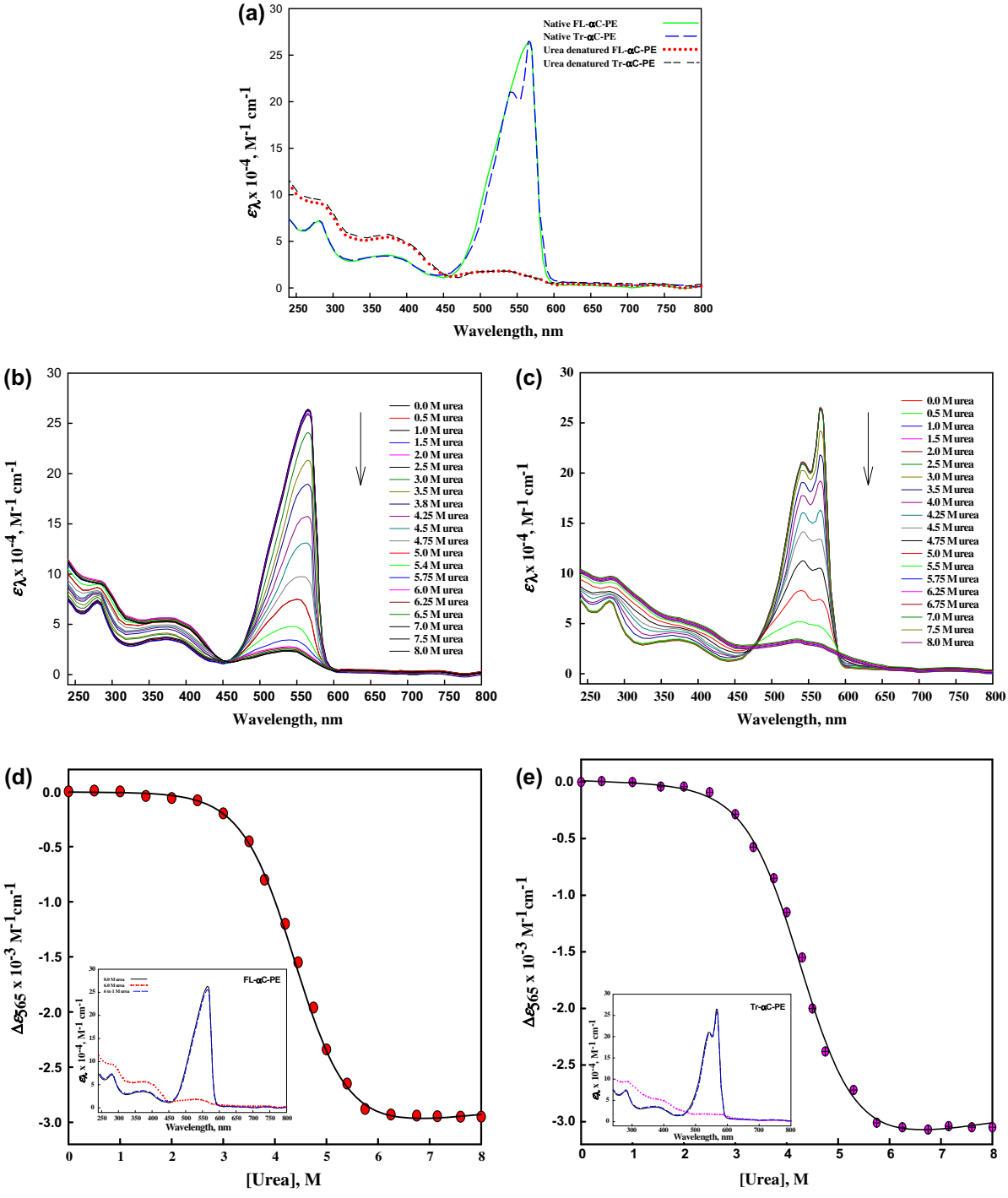

Figure 1. Absorption spectra of FL-αC-PE and Tr-αC-PE in the presence and absence of urea at pH 7.0 and 25 °C. (a) Absorption spectra of FL-αC-PE and Tr-αC-PE in the native and urea-induced denatured states. Changes in absorption spectra of (b) FL-αC-PE and (c) Tr-αC-PE as [urea] increases from .0 to 8.0 M. Denaturation curves of (d) FL-αC-PE and (e) Tr-αC-PE followed by observing changes in $\Delta\varepsilon_{565}$ as a function of [urea]. The insets in (d) and (e) show results of renaturation (see text).

a function of [urea]. Figure 1(b) and (c) shows spectra of FL-αC-PE and Tr-αC-PE at different urea concentrations, respectively. It is seen in this figure that successive reductions in the absorption of FL-αC-PE and Tr-αC-PE in the presence of urea were observed as the urea concentration increases. All these comprise faster decreases in the absorbance at 565 nm reflecting gradual reductions in absorption capability of the PEBs and their interactions with proteins. More significant decreases in absorbance are observed when the urea concentration is above 3.0 M. However, all these reductions in absorbance are attributed to PEBs and their interactions with the proteins, as reported earlier (Martinez-Oyanedel et al., 2004). Above 6 M of urea concentration, the peaks of both the proteins get vanished leaving very low absorption. Also, the two peaks of Tr-αC-PE gradually become common and widened as the concentration of urea is increased, and the protein gets denatured (Figure 1(c)). Thus, in denatured states, there is no separate identity of 565 or 542 nm peaks in Tr-αC-PE due to the gradual red and blue shift of the 542 and 565 nm peaks, respectively. This indicates that both proteins do not maintain their folded structures and interactions with the chromophores at these higher concentrations of urea. This loss in protein structure and its interaction with PEBs may also be due to less rigidity caused by destruction of hydrogen bonds and hydrophobic networks (Ma et al., 2007).

Figure 1(d) and (e) shows plots of $\Delta\varepsilon_{565}$ (difference in molar absorption coefficients at 565 nm in the presence and absence of urea) of FL-αC-PE and Tr-αC-PE as a function of [urea], respectively. These plots were analyzed for ΔG_D^0, m, and C_m values for each protein according to Equation (2). Result of this analysis is summarized in Table 1.

Both the FL- and Tr-αC-PE have a lone tryptophan at position 77 (numbering is according to the full length protein). This intrinsic fluorophore is buried and is at a distance of 17 Å from the PEB2 (Soni et al., 2010). After excitation at 287 nm, we have measured emission spectra of both proteins in the presence of different concentrations of urea at pH 7.0 and 25 ± .1 °C (see Figure 2(a) and (b)). As can be seen in Figure 2(a) and (b), when a protein is transferred from the native buffer to the denaturant solution, there is an expected red shift of the emission spectrum from 350 to 360 nm (Vivian & Callis, 2001). However, contrary to the expectation, the emission intensity is increased on denaturation (Vivian & Callis, 2001; White, 1958). This increase can be explained by invoking quenching phenomenon due to the presence of PEB2 near Trp77, which will decrease when the protein unfolds. We have exploited this phenomenon to follow urea-induced denaturation of FL- and Tr-αC-PEs. Values of emission intensity at 350 nm (F_{350}) of both proteins read from the spectra shown in Figure 2(a) and (b) were plotted as a function of [urea] (Figure 2(c) and (d)). These denaturation curves (Figure 2(c) and (d)) were analyzed for ΔG_D^0, m, and C_m values for each protein according to Equation (2). Result of this analysis is summarized in Table 1.

PEB has fluorescence property (Dammeyer & Frankenberg-Dinkel, 2006; French & Young, 1952; Liu et al., 2009). It has been shown that the covalently bonded PEBs to the protein polypeptide chain via thioether bonds have a strong emission spectrum in the wavelength region 500–600 nm, which vanishes on protein denaturation (Kupka & Scheer, 2008; Liu et al., 2009). After exciting FL-αC-PE and Tr-αC-PE at 479 nm, we have measured emission spectra of both proteins in the presence of different concentrations of urea at pH 7.0 and 25 °C. These spectra are shown in Figure 2(e) and (f) for FL-αC-PE and Tr-αC-PE, respectively. Figure 2(g) and (h) show the change in F_{573}, the fluorescence intensity of FL-αC-PE and Tr-αC-PE at 573 nm as a function of [urea], respectively. For each protein, urea-induced denaturation curves were analyzed for ΔG_D^0, m, and C_m values by fitting the entire denaturation curve according to Equation (2). The results of this analysis are shown in Table 1.

To see the effect of urea on the stability of FL-αC-PE and Tr-αC-PE in terms of secondary structure, we have measured the far-UV CD spectra of both proteins in the presence of different concentrations of urea. These measurements are shown in Figure 3(a) and (b). The insets in Figure 3(c) and (d) show the far-UV CD spectra of FL-αC-PE and Tr-αC-PE, respectively. Analysis of the far-UV CD spectrum of the native FL-αC-PE for the contents of α-helix and β-sheet yielded values of 73 and

Table 1. Stability parameters of FL-αC-PE and Tr-αC-PE associated with the urea-induced denaturation at pH 7.0 and 25 °C.*

	FL-αC-PE			Tr-αC-PE		
Probes	ΔG_D^0 (kcal mol^{-1} M^{-1})	m_u (kcal mol^{-1} M^{-1})	C_{mu} (M)	ΔG_D^0 (kcal mol^{-1} M^{-1})	m_u (kcal mol^{-1} M^{-1})	C_{mu} (M)
$\Delta\epsilon_{567}$	10.59 ± .47	2.45 ± .13	4.33 ± .67	9.69 ± .38	2.29 ± .13	4.24 ± .29
F_{350}	10.68 ± .14	2.51 ± .21	4.26 ± .93	9.51 ± .09	2.27 ± .15	4.19 ± .16
F_{573}	10.23 ± .21	2.37 ± .09	4.31 ± .09	9.13 ± .73	2.19 ± .77	4.21 ± .04
$[\theta]_{222}$	10.98 ± .12	2.47 ± .16	4.44 ± .43	9.89 ± .14	2.29 ± .41	4.32 ± .61

Note: *A ± with a value is a mean of errors from the average of three independent measurements.

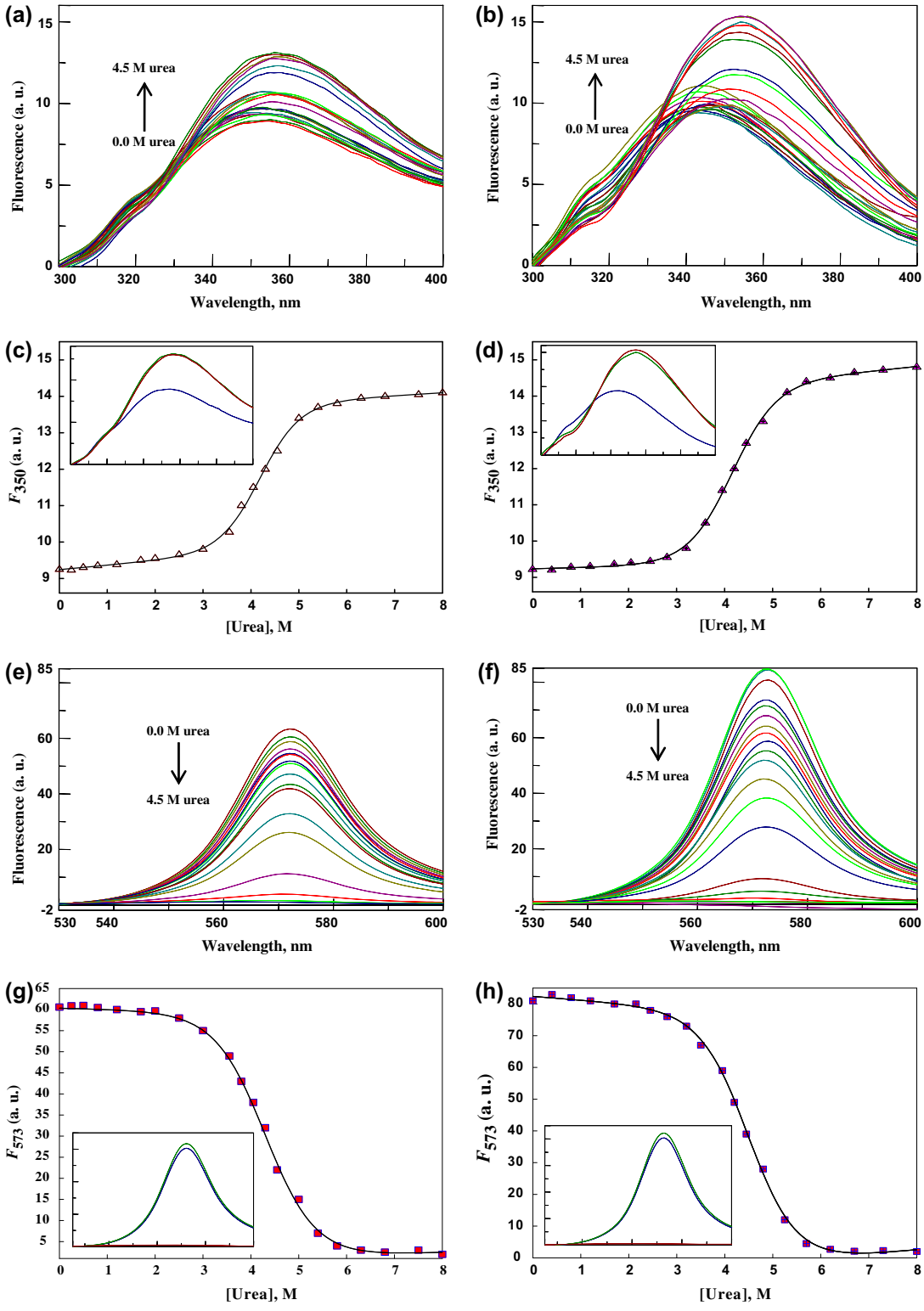

Figure 2. Fluorescence spectra of FL-αC-PE and Tr-αC-PE at pH 7.0 and 25 °C. (a) FL-αC-PE and (b) Tr-αC-PE were excited at 287 nm and emission spectra from 300 to 400 nm were recorded as function of [Urea]. Denaturation profiles of (c) FL-αC-PE and (d) Tr-αC-PE followed by observing changes in F_{350} as a function of urea concentration. The insets in (c) and (d) show results of renaturation experiments (see text). Emission spectra of (e) FL-αC-PE and (f) Tr-αC-PE in the presence of different urea concentrations; the wavelength of excitation was 479 nm. Changes F_{573} of (g) FL-αC-PE and (h) Tr-αC-PE as a function of [urea]. The insets in (g) and (h) show results of renaturation experiments (see text).

0%, respectively. Analysis of the far-UV CD spectrum of the Tr-αC-PE for the secondary structure gives 61 and 0% for the α-helix and β-structure, respectively, which are in excellent agreement with those determined by the X-ray diffraction studies (Chang et al., 1996; Soni et al., 2010).

Values of $[\theta]_{222}$ (probe for the secondary structure) in the presence of different concentrations of urea were determined from these CD spectra shown in Figure 3(a) and (b). Figure 3(c) and (d) show plots of $[\theta]_{222}$ vs. [urea] for FL-αC-PE and Tr-αC-PE, respectively. Each of these plots (denaturation curves) was analyzed for values of ΔG_D^0, m, and C_m by fitting the entire denaturation curve according to Equation (2). These stability parameters thus obtained are given in Table 1.

The analysis of transition curves (Figures 1–3) for the stability parameters, ΔG_D^0, m, and C_m (Table 1), according to Equation (2) is based on a few basic assumptions. First is that the urea-induced denaturations of the full length and truncated αC-PEs are reversible. To check the reversibility of denaturation, we have denatured FL-αC-PE and Tr-αC-PE by adding different concentrations of urea ([urea] ≥4.0 M). The urea-denatured protein was diluted with the native buffer to check the reversibility of denaturation at 6.0, 5.0, 4.0, and 1.0 M urea. After incubation of the denatured protein for a time enough for the completion of the renaturation process, optical spectra (absorption, fluorescence, and far-UV CD) were recorded. A spectrum of the renatured protein was then compared with that obtained during denaturation experiments at the same [urea]. It was observed that the spectral properties of the renatured protein in a given [urea] are identical to those obtained during denaturation experiments. Insets in Figures 1(d) and (e), 2(c), (d), (g) and (h), and 3(c) and (d) show the representative data which were obtained on denaturing the protein by 6.0 M urea and renaturing this denatured protein by diluting with the buffer to bring the denaturant

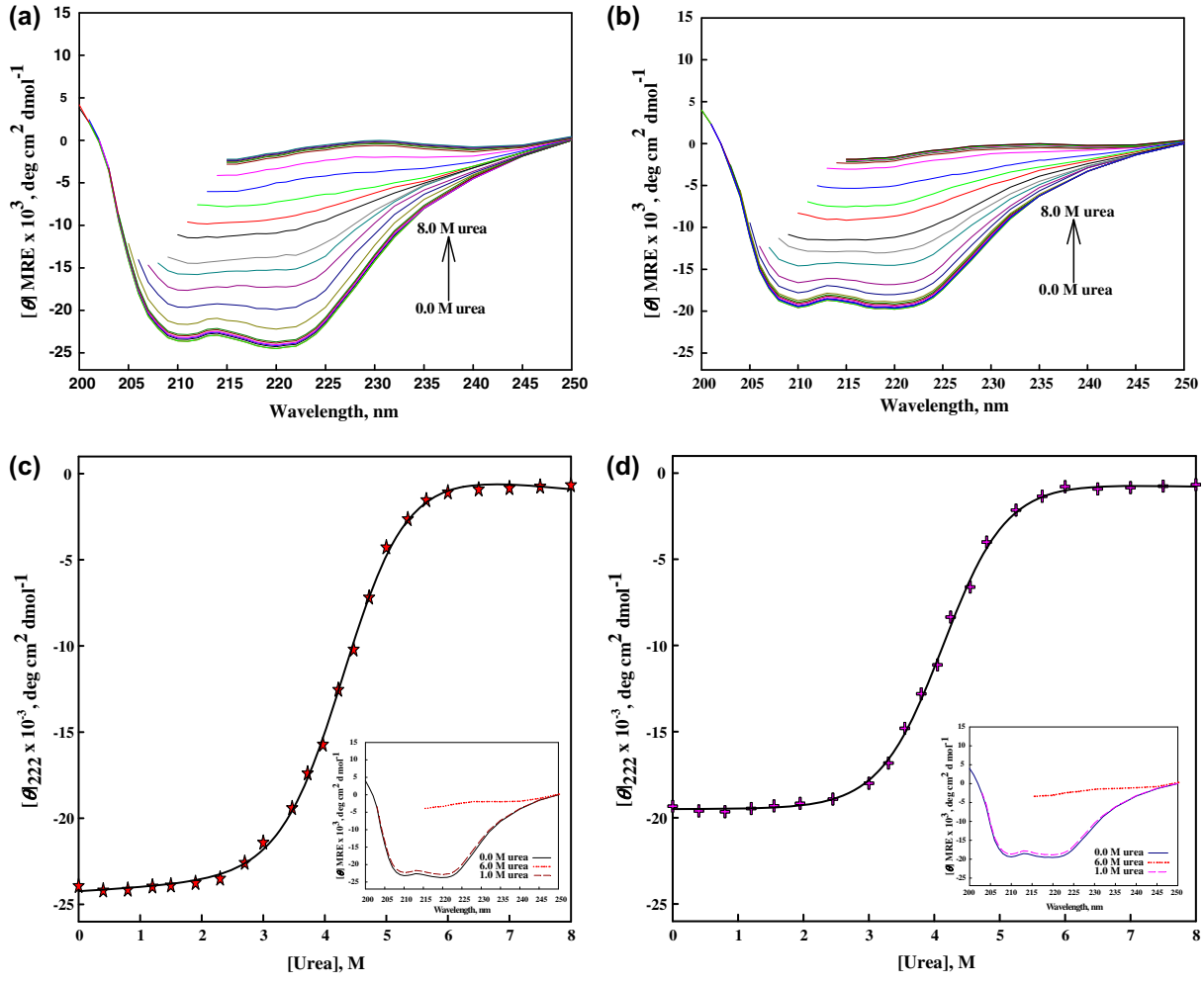

Figure 3. The far-UV CD spectra of FL-αC-PE and Tr-αC-PE at pH 7.0 and 25 °C. CD spectra of (a) FL-αC-PE and (b) Tr-αC-PE were recorded in the presence of urea concentration in the range .0–8.0 M. Denaturation curves of (c) FL-αC-PE and (d) Tr-αC-PE. The insets in (c) and (d) show renaturation results for the urea-denatured FL-αC-PE and Tr-αC-PE, respectively.

concentration to 1.0 M. It has been observed that the spectra of the protein in a given [urea] obtained from the denaturation and renaturation experiments were indistinguishable. The spectra of the denatured and renatured proteins are also compared with those of the native proteins. The coincidence of optical properties of the proteins obtained from denaturation and renaturation experiments led us to conclude that the urea-induced denaturation of FL-αC-PE and Tr-αC-PE is reversible.

The second assumption was that the urea-induced transition between N and D states is a two-state process. The most authentic criterion for a two-state behavior of the protein denaturation is to show that the calorimetric and van't Hoff enthalpy changes on denaturation are identical. We could not succeed to make differential scanning calorimetric measurements on Fl-αC-PE and Tr-αC-PE proteins due to the fact that the heat-denatured proteins formed aggregates. However, another test for the two-state behavior of protein denaturation is to show coincidence of the normalized sigmoidal curves of different physical properties induced by urea [26]. For this, transition curves of $\Delta\varepsilon_{565}$, F_{350}, F_{573}, and $[\theta]_{222}$ (Figures 1–3) were normalized with the help of Equation (3). These normalized curves are shown in Figure 4(a) and (b) for FL-αC-PE and Tr-αC-PE, respectively. Interestingly, all curves are precisely overlapping for both the proteins suggesting two-state mechanism. However, this is a necessary but not a sufficient criterion for a two-state behavior of protein denaturation (Tanford, 1968). Customarily, the observation of non-coincidence of normalized transition curves of different physical properties constitutes a proof of existence of stable intermediate(s) on the folding ↔ unfolding pathways (Tanford, 1968). On the contrary, basing their arguments on theoretical grounds, Dill and Shortle (1991) have shown that the non-coincidence of sigmoidal curves of two different physical properties is also observed for a two-state protein denaturation. Recently, Rahaman et al. (2013) pro-

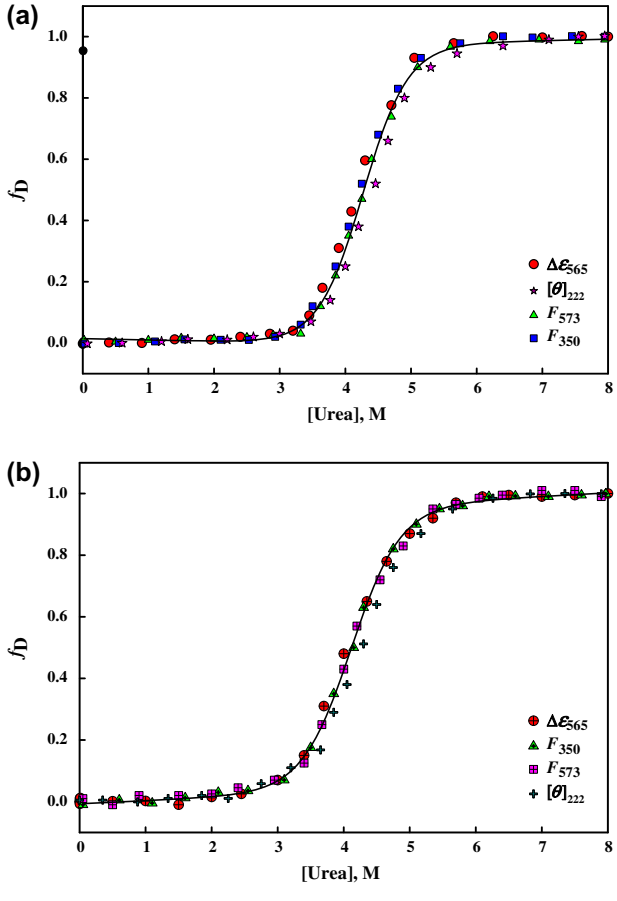

Figure 4. Normalized urea-induced denaturation curves of FL-αC-PE and Tr-αC-PE at pH 7.0 and 25 °C. Results obtained from denaturation curves of $\Delta\varepsilon_{565}$, F_{350}, F_{573}, and $[\theta]_{222}$ were used to construct plots of f_D of (a) FL-αC-PE and (b) Tr-αC-PE vs. [urea].

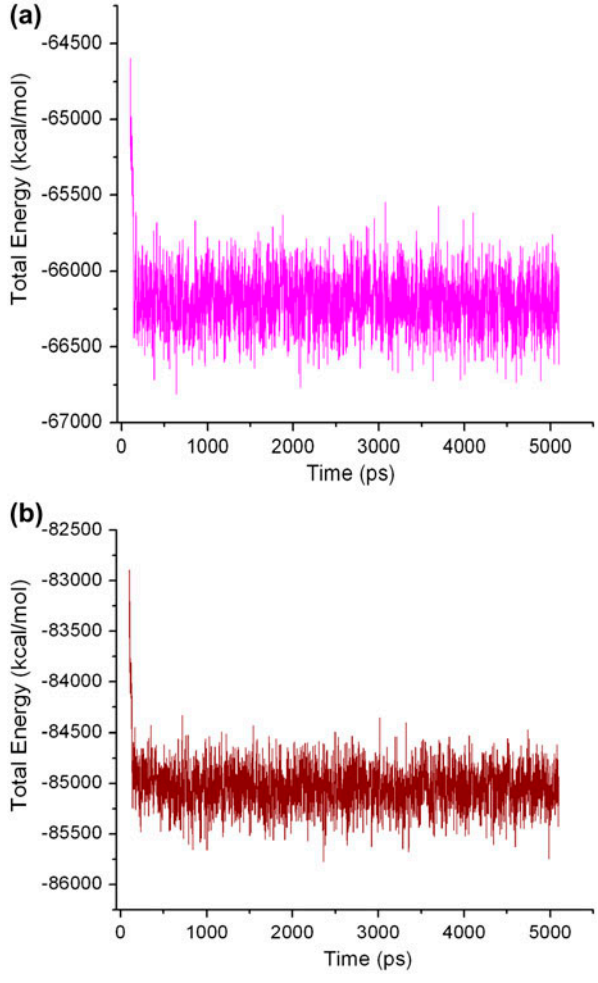

Figure 5. Total energy of the conformations. Total energy of the conformations for (a) Tr-αC-PE and (b) FL-αC-PE during the MD sampling process.

vided experimental evidence that this non-coincidence is consistent with two-state denaturation behavior.

In another approach for testing the two-state behavior of the urea-induced denaturation, ΔG_D^0 values of the protein are measured from sigmoidal curves of different structural properties, and it is shown that this thermodynamic property is independent of techniques (probes) used to monitor the denaturation (Bolen & Yang, 2000). Table 1 shows that the values of ΔG_D^0 of each protein measured by four different structural properties are, within experimental errors, identical. This overlap in ΔG_D^0 values suggests that the urea-induced denaturation of Fl-αC-PE and Tr-αC-PE is a two-state process.

Estimates of ΔG_D^0 from the denaturation curves depend not only on the mechanism of denaturation but also on the models describing the dependencies of the observed ΔG_D^0 on [urea]. There are three models to estimate ΔG_D^0 from the extrapolation of ΔG_D to 0 M urea (Aune & Tanford, 1969; Tanford, 1970). One model assumes that ΔG_D value varies linearly with [denaturant]. The one (binding model) assumes the presence of 'specific' binding sites for the chemical denaturant on the native and denatured protein molecules. In this model, dependence of ΔG_D on the [denaturant] is non-linear. The third model known as transfer-free energy model describes the dependence of ΔG_D on the transfer free energy of small model compounds for the protein groups from water to different concentrations of the chemical denaturant. It has been observed that the analysis of the same set of denaturation data using different models gives different values of ΔG_D^0 of a protein. However, we have used the linear free energy model for the analysis of denaturation curves of both FL-αC-PE and Tr-αC-PE (Figures 1–3), for it has supports of both theory (Schellman, 1978, 2002) and experiments (Ahmad & Bigelow, 1982; Bolen & Santoro, 1988; Gupta & Ahmad, 1999; Gupta et al., 1996; Pace, 1975).

From the above discussion it may be concluded that (1) FL-αC-PE and Tr-αC-PE undergo a two-state denaturation induced by urea, (2) values of ΔG_D^0 (protein stability) obtained from the analysis of their urea-induced denaturation curves according to Equation (2) are accurate, and (3) the stability of the full length and truncated proteins in terms of ΔG_D^0 are not very different (see Table 1).

To determine the difference in stability between FL-αC-PE and Tr-αC-PE, we have also performed MD simulation studies. Since the crystal structure and amino acid sequence of 31-residue long N-terminal segment of FL-αC-PE are unknown, we have used the determined structure of closely homologous α-Red algae phycoerythrin (αR-PE), which also belongs to an α-protein class (Chang et al., 1996). The sequence alignment of FL-αC-PE with αR-PE gives 94% sequence homology (Soni et al., 2010). Thus, it can be expected that αR-PE and FL-αC-PE have identical 3-D structure, for αR-PE (PDB code: 1LIA) and Tr- αC-PE (PDB code: 3MWN) have identical 3-D structures. Taking advantage of this and to support our experimental results, two MD simulations of length 5 ns were performed on the full length peptide (αR-PE) and truncated αC-PE (Tr-αC-PE) under explicit solvent conditions at 300 K. The AMBER program (Case et al., 2005) was used for simulations as it has been widely used to explore the conformational preferences of peptides/proteins.

Initially, a qualitative analysis on the thermodynamic properties (total energy and temperature) was performed to assess the stability and quality of the MD simulations performed. The constant average fluctuation of temperature around 300 K suggested stable and accurate nature of the MD simulations performed. The total energies of the sampled conformations of both proteins were further plotted as a function of simulation time and are pictorially depicted in Figure 5(a) and (b). The average total energy for Tr-αC-PE (Figure 5(a)) and FL-αC-PE

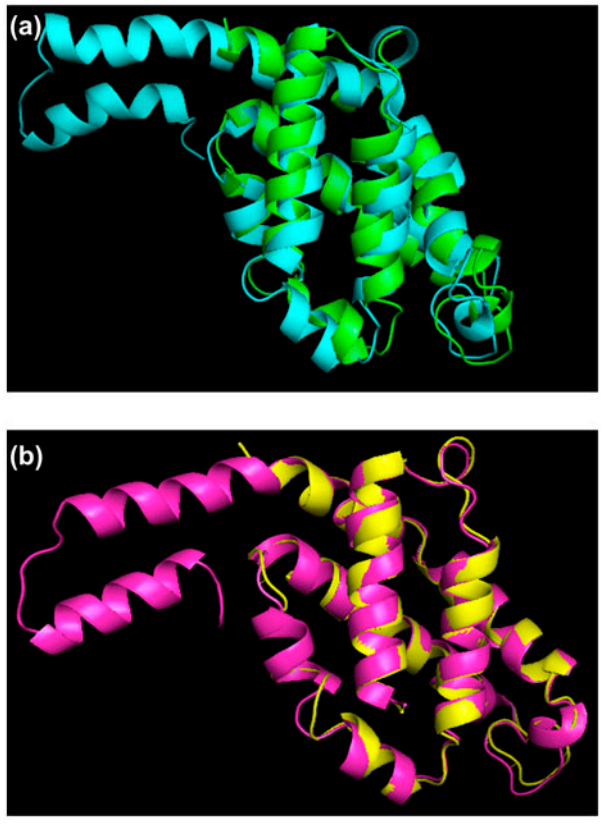

Figure 6. Overlay of conformations. (a) Overlay of the optimized conformations of Tr-αC-PE (in green) and FL-αC-PE (in light blue). (b) Overlay of the initial conformations of Tr-αC-PE (in yellow) and FL-αC-PE (in pink). All atoms of the proteins are represented in cartoon form.

(Figure 5(b)) was found to be around −66,220 and −85,090 kcal mol^{-1}, respectively.

The lowest energy structure of Tr-αC-PE and FL-αC-PE was further extracted from their respective MD trajectories using the PTRAJ module in AMBER. The root mean square deviation (RMSD) between optimized (lowest energy) structures of Tr-αC-PE and FL-αC-PE was 1.963 Å (Figure 6(a)), somewhat greater than those present between their initial structures (RMSD = .632 Å, Figure 6(b)), suggesting some structural changes in their conformations during simulations. Moreover, the RMSDs between the initial and final structures of FL-αC-PE and Tr-αC-PE were 1.844 and 1.385 Å, respectively (Figure 7(a) and (b)), suggesting the more structural deviation in case of FL-αC-PE. However, the overall pattern of the secondary features was almost preserved in the initial and optimized structures of both proteins. In terms of new interactions, two hydrogen bonds formed between Val4 and Val99, and Val4 and Arg37 were observed in case of FL-αC-PE.

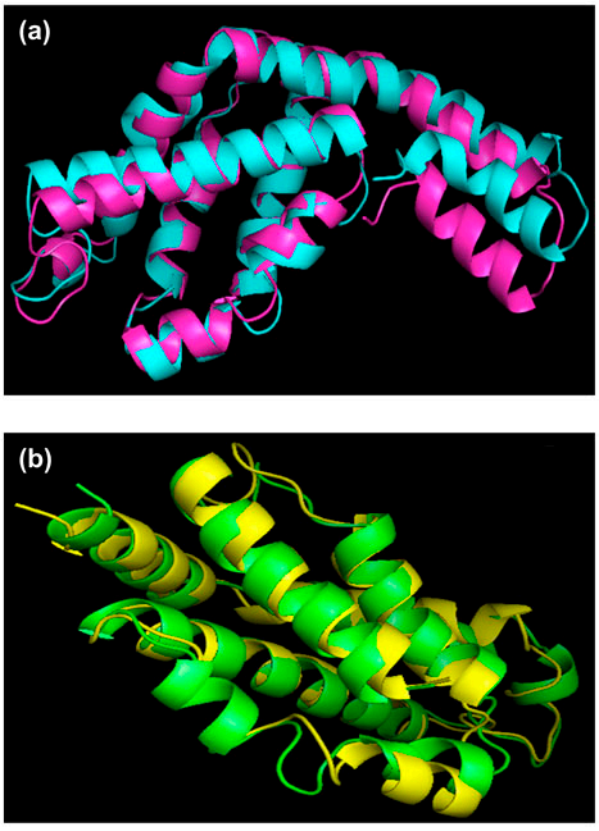

Figure 7. Overlay of initial and optimized conformations. (a) Overlay of the initial (in pink) and optimized (in light blue) conformations of FL-αC-PE. (b) Overlay of the initial (in green) and optimized (in yellow) conformations of Tr-αC-PE. All atoms of the proteins are represented in cartoon form.

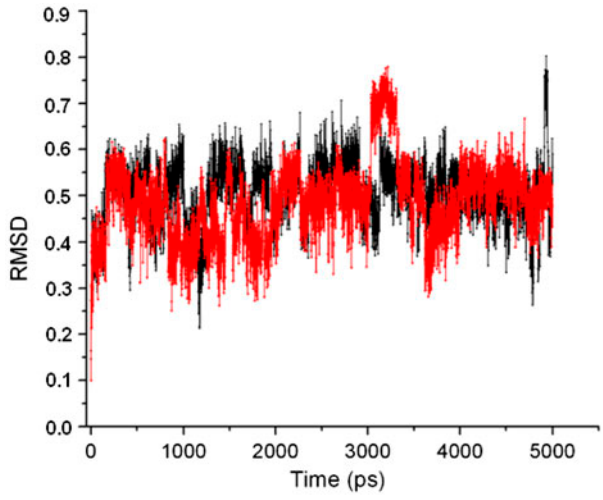

Figure 8. RMSDs (in Å) of the MD trajectories relative to their starting structures for Tr-αC-PE (in black) and FL-αC-PE (in red) computed using backbone atoms.

Finally, the RMSDs of the both MD trajectories calculated relative to their starting structures, considering their backbone atoms, were found to be less than 1 Å (Figure 8), and supported the stable nature of both proteins during the MD simulations.

Undoubtedly, the presence of additional residues in the N-terminal end of FL-αC-PE affects the overall geometry of the protein to some extent; but the retention of the main α-helical bundles in its structure illustrates the stability of this protein, and probably accounts for the retention of biological activity of Tr-αC-PE in the absence of these N-terminal residues.

Conclusions

FL-αC-PE and naturally truncated Tr-αC-PE devoid of 31 N-terminal residues were successfully isolated and purified. Truncation does not affect the interaction of PEBs with these proteins. Four different probes $\Delta\varepsilon_{565}$, F_{350}, F_{573}, and $[\theta]_{222}$ were used to monitor the effect of urea on FL-αC-PE and Tr-αC-PE to compare their stability. A very small difference in the values of ΔG_D^0 between FL-αC-PE and Tr-αC-PE was observed, for the full length protein is only ~1 kcal mol^{-1} more stable than the truncated protein. The 31-residue long N-terminal segment in the FL-αC-PE does not perturb the function of FL-αC-PE. Truncation has no effect on the mechanism of folding, for both proteins undergo a two-state transition between N and D states. Our MD simulation results show the stable nature of both variants (FL-αC-PE and Tr-αC-PE) and support the experimental observations that the biological activity is retained in the absence of these residues. This study

of the structure, function, and stability of FL-αC-PE and the naturally truncated Tr-αC-PE could be helpful for a better understanding of the mechanism of energy transfer in photosynthetic blue-green algae and other lower organisms.

Acknowledgments

The authors would like to express their acknowledgment to the Centre for high performance computing, an initiative support by the Department of Science and Technology of South Africa.

Funding

MIH and FA are thankful to the Department of Science and Technology for financial support [grant number SO/BB-0124/2010A]. KA is thankful to University Grant Commission for providing Maulana Azad National Fellowship.

References

Ahmad, F., & Bigelow, C. C. (1982). Estimation of the free energy of stabilization of ribonuclease A, lysozyme, alpha-lactalbumin, and myoglobin. *Journal of Biological Chemistry, 257*, 12935–12938.

Aune, K. C., & Tanford, C. (1969). Thermodynamics of the denaturation of lysozyme by guanidine hydrochloride. I. Dependence on pH at 25 degrees. *Biochemistry, 8*, 4579–4585.

Bolen, D. W., & Santoro, M. M. (1988). Unfolding free energy changes determined by the linear extrapolation method. 2. Incorporation of delta G degrees N-U values in a thermodynamic cycle. *Biochemistry, 27*, 8069–8074.

Bolen, D. W., & Yang, M. (2000). Effects of guanidine hydrochloride on the proton inventory of proteins: implications on interpretations of protein stability. *Biochemistry, 39*, 15208–15216.

Case, D. A., Cheatham, T. E. 3rd, Darden, T., Gohlke, H., Luo, R., Merz Jr., K. M., … Woods, R. J. (2005). The Amber biomolecular simulation programs. *Journal of Computational Chemistry, 26*, 1668–1688.

Chang, W. R., Jiang, T., Wan, Z. L., Zhang, J. P., Yang, Z. X., & Liang, D. C. (1996). Crystal structure of R-phycoerythrin from *Polysiphonia urceolata* at 2.8 Å resolution. *Journal of Molecular Biology, 262*, 721–731.

Cornejo, J., Beale, S. I., Terry, M. J., & Lagarias, J. C. (1992). Phytochrome assembly. The structure and biological activity of 2(R), 3(E)-phytochromobilin derived from phycobiliproteins. *Journal of Biological Chemistry, 267*, 14790–14798.

Dammeyer, T., & Frankenberg-Dinkel, N. (2006). Insights into phycoerythrobilin biosynthesis point toward metabolic channeling. *Journal of Biological Chemistry, 281*, 27081–27089.

Dill, K. A., & Shortle, D. (1991). Denatured states of proteins. *Annual Review of Biochemistry, 60*, 795–825.

French, C. S., & Young, V. K. (1952). The fluorescence spectra of red algae and the transfer of energy from phycoerythrin to phycocyanin and chlorophyll. *Journal of General Physiology, 35*, 873–890.

Glazer, A. N. (1982). Phycobilisomes: Structure and dynamics. *Annual Review of Microbiology, 36*, 173–198.

Gray, B. H., Lipschultz, C. A., & Gantt, E. (1973). Phycobilisomes from a blue-green alga *Nostoc* species. *Journal of Bacterioloy, 116*, 471–478.

Griogoriev, I. V. (1998). Simulated annealing for alpha-helical protein folding: Searches in vicinity of the 'Molten Globule' state. *Journal of Biomolecular Structure and Dynamics, 16*, 115–122.

Gupta, R., & Ahmad, F. (1999). Protein stability: Functional dependence of denaturational Gibbs energy on urea concentration. *Biochemistry, 38*, 2471–2479.

Gupta, R., Yadav, S., & Ahmad, F. (1996). Protein stability: Urea-induced versus guanidine-induced unfolding of metmyoglobin. *Biochemistry, 35*, 11925–11930.

Horng, J. C., Tracz, S. M., Lumb, K. J., & Raleigh, D. P. (2005). Slow folding of a three-helix protein via a compact intermediate. *Biochemistry, 44*, 627–634.

Kupka, M., & Scheer, H. (2008). Unfolding of C-phycocyanin followed by loss of non-covalent chromophore-protein interactions 1. Equilibrium experiments. *Biochimica et Biophysica Acta, 1777*, 94–103.

Liu, L. N., Su, H. N., Yan, S. G., Shao, S. M., Xie, B. B., Chen, X. L., … Zhang, Y. Z. (2009). Probing the pH sensitivity of R-phycoerythrin: Investigations of active conformational and functional variation. *Biochimica et Biophysica Acta, 1787*, 939–946.

Ma, Y., Xie, J., Zhang, C., & Zhao, J. (2007). Three-stage refolding/unfolding of the dual-color beta-subunit in R-phycocyanin from *Polysiphonia urceolata*. *Biochemical and Biophysical Research Communications, 352*, 787–793.

MacColl, R. (1998). Cyanobacterial phycobilisomes. *Journal of Structural Biology, 124*, 311–334.

MacColl, R. (1999). Studies on R-phycoerythrins from two Antarctic marine red algae and a mesophilic red alga. *Polar Biology, 22*, 384–388.

MacColl, R. (2004). Allophycocyanin and energy transfer. *Biochimica et Biophysica Acta, 1657*, 73–81.

Martinez-Oyanedel, J., Contreras-Martel, C., Bruna, C., & Bunster, M. (2004). Structural-functional analysis of the oligomeric protein R-phycoerythrin. *Biological Research, 37*, 733–745.

Modig, K., Kurian, E., Prendergast, F. G., & Halle, B. (2003). Water and urea interactions with the native and unfolded forms of a beta-barrel protein. *Protein Science, 12*, 2768–2781.

Pace, C. N. (1975). The stability of globular proteins. *CRC Critical Reviews in Biochemistry, 3*, 1–43.

Pace, C. N. (1986). Determination and analysis of urea and guanidine hydrochloride denaturation curves. *Methods in Enzymology, 131*, 266–280.

Pace, C. N. (1995). How to measure and predict the molar absorption coefficient of a protein. *Protein Science, 4*, 2411–2423.

Parmar, A. (2010). Allophycocyanin from a local isolate *geitlerinema* sp. a28 dm (cyanobacteria): A simple and efficient purification process. *Journal of Phycology, 46*, 285–289.

Parmar, A. (2011). Characterization of an intact phycoerythrin and its cleaved 14 kDa functional subunit from marine cyanobacterium *Phormidium* sp. A27DM. *Process Biochemistry, 46*, 1793–1799.

Parmar, A., Singh, N. K., Kaushal, A., Sonawala, S., & Madamwar, D. (2011). Purification, characterization and comparison of phycoerythrins from three different marine cyanobacterial cultures. *Bioresource Technology, 102*, 1795–1802.

Rahaman, H., Khan, M. K. A., Hassan, M. I., Islam, A., & Ahmad, F. (2013). Evidence of non-coincidence of normalized sigmoidal curves of two different structural properties for two-state protein folding/unfolding. *Journal of Chemical Thermodynamics, 58*, 351–358.

Royer, C. A. (2006). Probing protein folding and conformational transitions with fluorescence. *Chemical Reviews, 106*, 1769–1784.

Schellman, J. A. (1978). Solvent denaturation. *Biopolymers, 17*, 1305–1322.

Schellman, J. A. (2002). Fifty years of solvent denaturation. *Biophysical Chemistry, 96*, 91–101.

Shah, V., Garg, N., & Madamwar, D. (2001). Record of the marine cyanobacterium from the rocky shores of Bet-Dwarka and Okha, India. *Acta Botanica Malacitana, 26*, 188–193.

Singh, N. K., Parmar, A., & Madamwar, D. (2009). Optimization of medium components for increased production of C-phycocyanin from *Phormidium ceylanicum* and its purification by single step process. *Bioresource Technology, 100*, 1663–1669.

Soni, B. R., Hasan, M. I., Parmar, A., Ethayathulla, A. S., Kumar, R. P., Singh, N. K., … Singh, T. P. (2010). Structure of the novel 14 kDa fragment of alpha-subunit of phycoerythrin from the starving cyanobacterium *Phormidium tenue*. *Journal of Structural Biology, 171*, 247–255.

Tanford, C. (1968). Protein denaturation. *Advances in Protein Chemistry, 23*, 121–282.

Tanford, C. (1970). Protein denaturation. C. Theoretical models for the mechanism of denaturation. *Advances in Protein Chemistry, 24*, 1–95.

Vivian, J. T., & Callis, P. R. (2001). Mechanisms of tryptophan fluorescence shifts in proteins. *Biophysical Journal, 80*, 2093–2109.

White, A. (1958). Effect of pH on fluorescence of tyrosine, tryptophan and related compounds. *Biochemistry, 71*, 217–220.

Wilbanks, S. M., de Lorimier, R., & Glazer, A. N. (1991). Phycoerythrins of marine unicellular cyanobacteria. III. Sequence of a class II phycoerythrin. *Journal of Biological Chemistry, 266*, 9535–9539.

Yokono, M., Akimoto, S., Koyama, K., Tsuchiya, T., & Mimuro, M. (2008). Energy transfer processes in *Gloeobacter violaceus* PCC 7421 that possesses phycobilisomes with a unique morphology. *Biochimica et Biophysica Acta, 1777*, 55–65.